Loss of human Greatwall results in G2 arrest and multiple mitotic defects due to deregulation of the cyclin B-Cdc2/PP2A balance.

Andrew Burgess, Suzanne Vigneron, Estelle Brioudes, Jean-Claude Labbé, Thierry Lorca, Anna Castro

Loss of human Greatwall results in G2 arrest and multiple mitotic defects due to deregulation of the cyclin B-Cdc2/PP2A balance

Andrew Burgess, Suzanne Vigneron, Estelle Brioudes, Jean-Claude Labbé, Thierry Lorca*[1] and Anna Castro*[1]

BIOLOGICAL SCIENCES: Cell Biology

Running title: Human Greatwall controls mitosis through PP2A

Key Words: Greatwall, PP2A, cyclin B-Cdc2, Human Cells, SAC

Universités Montpellier 2 et 1, Centre de Recherche de Biochimie Macromoléculaire, CNRS UMR 5237, IFR 122, 1919 Route de Mende, 34293 Montpellier cedex 5, France

Phone 33 4 67 61 33 30

Fax 33 4 67 52 15 59

*Corresponding author E-mails: anna.castro@crbm.cnrs.fr and thierry.lorca@crbm.cnrs.fr

[1]Both authors contributed equally to this work

ABSTRACT

This paper shows that the functional human orthologue of Greatwall protein kinase (Gwl) is the "Microtubule Associated Serine/Threonine kinase-Like" protein, MAST-L. This kinase promotes mitotic entry and maintenance in human cells by inhibiting PP2A, a phosphatase that dephosphorylates cyclin B-Cdc2 substrates. The complete depletion of Gwl by siRNA arrests human cells in G2. When the levels of this kinase are only partially depleted, however, cells enter into mitosis with multiple defects and fail to inactivate the spindle assembly checkpoint (SAC). The ability of cells to remain arrested in mitosis by the SAC appears to be directly proportional to the amount of Gwl remaining. Thus, when Gwl is only slightly reduced, cells arrest at prometaphase. More complete depletion correlates with the premature dephosphorylation of cyclin B-Cdc2 substrates, inactivation of the SAC and subsequent exit from mitosis with severe cytokinesis defects. These phenotypes appear to be mediated by PP2A as they could be rescued by either a double Gwl/PP2A knockdown or by the inhibition of this phosphatase with okadaic acid (OA). These results suggest that the balance between cyclin B-Cdc2 and PP2A must be tightly regulated for correct mitotic entry and exit and that Gwl is crucial for mediating this regulation in somatic human cells.

\body

INTRODUCTION

In eukaryotic cells, the mitotic state is maintained by the mitotic kinase cyclin B-Cdc2. Historically, mitotic entry and exit was thought to be the direct consequence of cyclin B-Cdc2 activation and inactivation respectively (1). Recent results have expanded this model to include phosphatases (2). Specifically, recent evidence indicates that PP2A is responsible for

dephosphorylation of cyclin B-Cdc2 substrates and that the regulation of this dephosphorylation is required in mitotic entry and exit (3). This suggests a new model in which the balance between cyclin B-Cdc2 and PP2A controls mitotic entry and exit. Thus, during G2 PP2A activity is high and cyclin B-Cdc2 activity low, thereby preventing phosphorylation of mitotic substrates, whereas, at mitotic entry the balance flips allowing entry into mitosis. The mechanisms controlling cyclin B-Cdc2 activity have been largely described (4). Briefly, cyclin B-Cdc2 is inhibited during G2 by the inhibitory phosphorylation of Cdc2 on threonine 14 and tyrosine 15 by Wee1 and Myt1 kinases. Upon mitotic entry these are removed by the Cdc25 phosphatase (4). Finally, at mitotic exit cyclin B-Cdc2 is inhibited by the ubiquitin-dependent degradation of its regulatory subunit cyclin B (5). Unlike cyclin B-Cdc2 regulation, very little is known about the mechanisms controlling PP2A activity during mitosis, and therefore our understanding of G2 and mitosis is incomplete.

Recently, Greatwall (Gwl) a new critical mitotic regulator has been discovered in Drosophila (6, 7). It is a member of the AGC family of serine/threonine kinases that phosphorylates substrates on S/T residues encircled by basic amino acids. (7). Work done in Xenopus egg extracts suggested that Gwl promoted mitotic entry by controlling the auto-amplification loop of cyclin B/Cdc2 (8, 9). However it has been recently demonstrated that the main role of this kinase is not the regulation of cyclin B-Cdc2 activity but the inhibition of PP2A, the phosphatase that de-phosphorylates cyclin B-Cdc2 substrates (10, 11).

Despite the critical roles of Gwl in mitosis, the functional human orthologue of this kinase is currently unknown. The human protein with the closest homology to Drosophila and Xenopus Gwl is the Microtubule Associated Serine/Threonine kinase Like (MAST-L) (50,2% and 65.7% of sequence homology respectively) (Figure S1). In addition to the high homology of MAST-L with the other members of the Gwl family, it also contains a very long T-loop (>500 amino acids) that separates the kinase subdomains VII and VIII, a particular feature exclusive to Gwl kinases. In

contrast, although MAST-L was first classified as a member of the MAST family, it contains very little homology to any of the MAST kinases. All the members of the MAST family are large enzymes (1309-2444 amino acids) with a short T-loop (31 amino acids for MAST1), and contain a PDZ domain in the C terminus. However, MAST-L has minimal homology to MAST proteins (10,4% with MAST1), and no PDZ domain, suggesting that it is not a true member of the MAST family.

Very little is known about the role of MAST-L in human cells, with only two publications to date. Both of these publications focus on the role of MAST-L in Autosomal Dominant Thrombocytopenia showing that a single point mutation (E167D) in the N-terminal kinase domain correlates with this syndrome (12), while transient knockdown in zebrafish results in a reduction of circulating thrombocytes (13).

In the present study, we verified that MAST-L is the functional human orthologue of Gwl. Using siRNA knockdown of hGwl we show in human cells that this kinase mediates mitotic entry and maintains the mitotic state by inhibiting PP2A and thus, keeping the correct equilibrium between cyclin B-Cdc2 and PP2A.

RESULTS

MAST-L is the functional human homologue of Xenopus Greatwall

To analyse the role of Greatwall in human cells, we cloned the closest related human protein to the Drosophila and Xenopus Greatwall, the Microtubule Associated Serine/Threonine Kinase-Like protein (MAST-L) (12). Our previous results demonstrated that the depletion of Greatwall from mitotic egg extracts induced the loss of the mitotic state. To check whether MAST-L corresponds to the Greatwall orthologue, we translated MAST-L in “M-phase frog egg extracts” (CSF extracts) and tested its capacity to rescue the loss of endogenous Greatwall. The expression, at endogenous levels, of wild type MAST-L in these CSF extracts completely rescued the mitotic

state (Fig. S2A). However, expression of a kinase-dead mutant of MAST-L failed to rescue, indicating that MAST-L is the functional ortologue of Greatwall. Thus, from now, it will be referred to as human Greatwall (hGwl) in this manuscript.

We next analysed by western blot the expression of the endogenous human protein in Hela cells. Our antibodies clearly recognised and specifically immunoprecipitated a band around 110 KDa, the expected molecular weight of hGwl (Fig. S2B). The levels of hGwl appeared to be constant throughout the cell cycle (Fig. 1A and Fig. S2C and D). However a lower electrophoretic mobility of this protein appeared as cells entered mitosis, was maximal in prometaphase and disappeared by anaphase (Fig. 1A). This lower mobility was induced by phosphorylation as λ-Phosphatase treatment reversed the shift (Fig. S2E).

Previously in Drosophila, Gwl was identified as a nuclear protein (7). However, while hGwl is mostly present in the nucleus of interphase human cells, we also noted a consistent partial localization in the cytoplasm and at the centrosomes during G1, S and G2 phases (Fig. 1B). The centrosomal hGwl appeared to surround γ-tubulin, indicating that hGW is localized around the pericentriolar material (Fig. 1C). As cells entered mitosis, hGwl concentrated at the poles of the spindle and emanated out along the microtubule spindle fibres (Fig. 1B and C). At anaphase the protein started to leave the mitotic spindle and becomes more diffuse in the cytoplasm. Finally, from telophase to cytokinesis, once the nuclear membrane reformed, most of the hGwl is localised in the nucleus, but a small fraction stayed at the cleavage furrow where it remained on the midzone microtubules although occasionally it was also observed at the mid-body (Fig. 1C). We detected a similar localization of this protein in in U2OS cells and by using two different antibodies, one against the full-length protein and the other against the last 12 C-terminal amino acids of hGwl.

hGwl knockdown promotes G2 arrest and mitotic defects in Hela cells that can be rescued by the knockdown or the inhibition of PP2A by OA

It has been previously shown that depletion of Gwl in Xenopus egg extracts both prevents mitotic entry and promotes mitotic exit (8, 10, 11).

To investigate the role of hGwl in human cells we induced its knockdown by siRNA in Hela cells. The levels of hGwl decreased in a dose-dependent manner when increasing doses of the hGW siRNA were used, with an almost complete knockdown of this protein after 48h with 100 nM dose of this siRNA, both by western blot (Fig.1D) and immunofluorescence (Fig. 1E).

We next analysed if knockdown of hGwl in cells resulted in any alteration in mitotic entry or in the maintenance of the mitotic state. Flow Cytometry analysis (FACS) after a 48 h siRNA treatment of asynchronous cells produced an accumulation (40%) of cells with a 4n DNA content and a notable increase of sub-diploid cells, indicating that the knockdown of hGwl induced G2/M cell cycle dependent defects and an increase in cell death (Fig. 1F).

Immunofluorescence analysis revealed that the accumulation of cells with 4n DNA content was not primarily due to an increase in the mitotic index (6,9% of mitotic cells from 40% of knockdown cells containing 4n DNA content), but due most likely to an increase in multinuclear cells (Fig. S3A and Fig.1G, vii), although some of these 4n cells could be arrested in G2.

The multinuclear cells are likely the result of an improper cytokinesis, as there were numerous signs of incorrect mitotic divisions with many cells displaying DNA bridges connecting daughter cells (Fig. S3A and Fig. 1G, vi). Finally, in some cases we noticed a more severe cytokinesis phenotype with one daughter cell containing the complete DNA content whereas the other was completely devoid of chromatin (Fig. 1G, viii).

In addition to multinuclear cells, we also observed significant chromosome abnormalities in mitotic cells. Metaphase cells showed either a mass of undercondensed chromatin that was scattered along the spindle (Fig. 1G, iii) or condensed chromosomes that did not correctly congress to the metaphase plate (Fig. 1G, v). A very low number of anaphases were observed, but those that were present showed multiple lagging chromosomes and chromosome bridges (Fig. 1G,

iv). No major defects were observed in the spindle although some were longer and appeared to have a lower number of microtubules (Fig. 1G, iii). These phenotypes were specific to Gwl knockdown as similar phenotypes were observed with two other siRNAs targeting different regions of hGwl mRNA (Fig. S3B and C).

The mitotic defects observed after hGwl knockdown are indicative of a premature exit from mitosis. To assess whether this was the case, time-lapse videos were performed on synchronised HeLa cells stably expressing EB3-GFP and H2B-CherryFP. Scramble siRNA treated cells progressed through mitosis normally (Fig. 2A, video S1). One of the major phenotypes observed at a 50 nM-dose of hGwl siRNA was a decrease in the total number of cells that were able to perform mitosis during the experiment (65% versus 80% in controls), suggesting that some cells were arrested at G2, similar to what has been described in Xenopus egg extracts (11). However, most cells were still able to enter into mitosis, albeit with numerous mitotic defects. Although the mitotic spindle structure did not contain any observable defects, in some cases the spindle rotated dynamically within the cell performing several rotations (Fig. 2A, video S3, Fig.S4). Moreover, some knockdown cells showed normal formation of the metaphase plate, however chromosomes segregated incorrectly resulting in the formation of DNA bridges (Fig. 2A, “Segregation Defects” and video S2). Other cells displayed clear defects in chromosome congression showing a high number of lagging chromosomes that were constantly present at the spindle poles and never correctly congressed to the metaphase plate. Many of these cells arrested during metaphase for long periods and finally died (Fig. 2A, “Metaphase Arrest”, video S3), whereas, others first delayed during metaphase and subsequently performed an aberrant anaphase with significant chromosome segregation and cytokinesis defects (Fig. 2A, “Metaphase Delay”, video S4). This delay/arrest in metaphase appeared to be mediated by the SAC as the SAC proteins BubR1 and Aurora B were clearly localized at the kinetochores in hGwl depleted cells (Fig. 2B). Finally, a subpopulation of cells displayed the most severe mitotic phenotype, in which cells entered and

exited mitosis prematurely without forming a metaphase plate and with severe chromosome segregation defects (Fig. 2A, “No Metaphase”, video S5). In these cells a cytokinesis furrow was formed and attempted to pinch through the DNA (Fig. S5), promoting the formation of multiple DNA bridges that were resolved by the cell rejoining and the formation of a multinuclear cell (Fig. 2A, “No Metaphase”, video S5).

Comparing the different phenotypes (“Segregation Defects”, “Metaphase Arrest”, “Metaphase Delay” and “No Metaphase”) against the time spent in mitosis, we noticed that all hGwl knockdown cells had an increased transit time through mitosis. Mitotic length in the “Metaphase Arrest” and “Metaphase Delay” phenotypes was four times longer compared to those of control cells. However, mitotic length in the “Segregation Defects” and “No Metaphase Plate” phenotypes was only twice that of controls (Fig. 2C), suggesting that despite the total absence of chromosome alignment, cells displaying a “No Metaphase Plate” phenotype were unable to maintain the mitotic state. No difference was observed in spindle rotation between the various subpopulation of hGwl-depleted cells, although, cells that maintained prolonged SAC activity were more likely to rotate. Thus, similar to Xenopus extracts, one of the major phenotypes of hGwl knockdown is a premature exit from mitosis. The knockdown of hGwl at a 50 nM-dose induced a variety of phenotypes probably due to the intrinsic heterogeneity of the siRNA transfection procedure. To try to separate the various phenotypes we repeated the experiment using various concentrations of hGwl siRNA (25, 50 and 100 nM). As the concentration of siRNA increased, there was a shift from cells that maintained the mitotic state (cells displaying the phenotypes “Segregation Defects”, “Metaphase Arrest” and the “Metaphase Delay”) towards cells incapable of maintaining mitosis (cells displaying the “No Metaphase Plate” phenotype) (Fig. 3A). Accordingly mitotic length decreased concomitantly with the increasing siRNA concentration (Fig. 3B).

Furthermore, as the dose of siRNA increased, there was a significant delay in the time of mitotic entry (Fig 3C), suggesting that cells were arrested in G2. To assess this issue in more detail,

synchronized cells were analyzed by 2 dimensional FACS (Fig. 3D). Both scramble and hGwl siRNA treated cells transited S and entered G2 phase with similar kinetics, indicating that hGwl is not critical for S phase progression. Entry into mitosis in scramble cells began at 8 h peaking at 9 h post-thymidine release. In contrast, there was a clear impairment in the ability of hGwl depleted cells to enter mitosis, with almost 3 times more (7.8% vs 20.9%) mitotic cells present in the scramble treated mitotic captured (nocodazole) 10 h time-point. Thus, at the highest dose of hGwl siRNA, cells arrest in G2.

It has been recently shown that the inhibition of the PP2A phosphastase activity is required to allow the phosphorylation of cyclin B-Cdc2 substrates, which promotes entry and maintains mitosis (3, 10, 11). Therefore, we next analysed the capacity of these cells to phosphorylate the different cyclin B-Cdc2 substrates at the different doses of siRNA (Fig. 3E). As most cells treated with a dose of 25 nM of siRNA arrest in mitosis after nocodazole treatment, we only observed a slight decrease in the levels of phosphorylation of cyclin B-Cdc2 substrates. However, at the higher doses of 50 and 100 nM, the phosphorylation levels of cyclin B-Cdc2 substrates were significantly reduced. This is most likely a result of the G2 arrest, although a partial degradation of cyclin B was also observed, probably as a result of cells that entered and subsequently slipped out of mitosis. In agreement with these results, we observed only a slight decrease in the immunostaining of cyclin B-Cdc2 substrates in mitotic hGwl-depleted cells (Fig. 3F), whereas a significant decrease in this signal was observed when cells prematurely exited mitosis (note decondensed DNA in the presence of a mitotic spindle). This decrease in the phosphorylation pattern of cyclin B-Cdc2 substrates was specific to hGwl knockdown as it was mostly rescued by the concomitant transfection of a siRNA-resistant plasmid encoding Xenopus Gwl (Fig. S6).

To assess if the decrease in cyclin B-Cdc2 substrate phosphorylation after hGW knockdown could be the consequence of an increase in PP2A activity due to a loss of hGW, we performed a double hGwl-PP2A siRNA knockdown (Fig. 3G). As expected, hGwl knockdown decreased the cyclin B-

Cdc2 substrate phosphorylation by 80% in nocodazole captured cells. When PP2A siRNA knockdown was performed, we noticed that the general substrate phosphorylation pattern was partially decreased compared to the scramble siRNA. This decrease is probably due to the 15% increase in cell death induced by PP2A depletion. Importantly, the double hGwl/PP2A knockdown rescued the general phosphorylation pattern of cyclin B-Cdc2 substrates from 20% to 64%. These results indicate that the hGwl knockdown phenotype is likely mediated by increased PP2A activity. However, it is possible that the knockdown of PP2A could promote a pleiotropic effect in other phases of the cell cycle (14). Thus, to more specifically investigate the role of Gwl in the regulation of PP2A activity at mitotic entry, we analysed if the inhibition of this phosphatase by OA could rescue the G2 arrest, the most severe phenotype observed in hGwl knockdown cells. Cells transfected with 100 nM of hGwl siRNA, were synchronised in G1/S phase, treated with OA and followed by time-lapse microscopy. The addition of OA at the end of S phase promoted a small but consistent advance in mitotic entry in scramble (SC) transfected cells (SC cells entered at an average time of 10 h 20 min after release versus 9 h 35min in OA treated cells) (Fig. 3H). As previously observed, hGwl knockdown cells delayed or arrested for a significant time in G2 (mean time of mitotic entry 12 h 12 min with significant number of cells arrested in G2 for as long as 20 hours post-release) (video S6). Importantly, OA treatment rescued the G2 delay/arrest induced by hGwl knockdown and cells entered into mitosis with similar kinetics as control cells (mean-time of mitotic entry 9 h 45 min versus 9 h 35 min in OA treated SC control cells) indicating that G2 arrest was mediated by an increased PP2A activity (video S7).

DISCUSSION

Historically, mitotic entry and exit was thought to be directly equivalent to cyclin B-Cdc2 activation and inactivation respectively, while the activity of the phosphatases required for cyclin B/Cdc2 substrate dephosphorylation during mitosis was thought to be constant. According to this hypothesis the large increase in cyclin B/cdc2 activity was sufficient to over-come the background

dephosphorylation of mitotic substrates, thereby promoting mitotic entry. Similarly, inactivation of the cyclin B-Cdc2 complex by cyclin B degradation was sufficient to trigger mitotic exit. However, recent data from our and other laboratories has demonstrated that PP2A is highly regulated during mitotic entry and exit (3, 10, 11). Therefore the old cell cycle model now must be update to include a new regulator of mitosis that modulates PP2A during this phase of the cell cycle. In this work we demonstrate that Gwl is this critical and evolutionally conserved new regulator of PP2A in human cells.

Greatwall is a novel kinase whose role is essential in Xenopus egg extracts to promote mitotic entry and to maintain the mitotic state (8, 10, 11). Here we identified MAST-L as the functional human orthologue of Gwl and demonstrated that its role is evolutionary conserved from Xenopus to human cells. During mitotic division, there is a highly regulated balance between cyclin B-Cdc2 and PP2A and this balance dictates the phosphorylation level of mitotic substrates. The regulation of this balance, performed by Gwl-dependent inhibition of PP2A, is essential to allow the correct entry into and exit from mitosis. Accordingly, the phenotypes observed after hGwl knockdown likely reflect the differential phosphorylation pattern of cyclin B-Cdc2 substrates. Thus, cells lacking hGwl have a fully active PP2A that will completely dephosphorylate cyclin B-Cdc2 substrates preventing cells from entering mitosis. Cells in which hGwl is partially present show an incomplete inactivation of PP2A. If this inactivation is sufficient, then cells can enter into mitosis, but display only a partial phosphorylation of the different mitotic substrates of cyclin B-Cdc2. Depending on the level of cyclin B-Cdc2-substrate phosphorylation, cells will display different mitotic defects such as improper chromosome congression or spindle rotation, which in some cases leads to a permanent prometaphase arrest by the SAC while in others mitotic slippage. In this regard, other reports described the presence of similar mitotic defects due to a partial inhibition of cyclin-Cdk activity (15-17). For example, siRNA knockdown of cyclin A results in improper chromosome congression and spindle rotation (15). Moreover, the inhibition of cyclin B-

Cdc2 activity in mitotic cells also induced mitotic slippage resulting in severe cytokinesis defects (17-19).

The exact mechanism of how Gwl regulates PP2A activity is currently unknown, although we previously demonstrated that xGwl can bind with PP2A/A and /C (11). PP2A itself is a complicated ternary complex comprising of a catalytic subunit (C), a scaffold subunit (subunit A) and a regulatory B subunit (14). The substrate specificity of the PP2A complex is thought to be conferred by the B subunit that include the B55 (B), B56 (B') and B72/130 (B''), with each also containing multiple isoforms. Recently PP2A-B55∂ was identified as a key phosphatase responsible for removing cyclin B/cdc2 phosphorylations (3). There are several possible phosphorylation sites in B55∂, suggesting that this complex could be regulated by phosphorylation, perhaps by Gwl itself.

It is clear from our work and others that the classical cyclin/cdk cell cycle model, must be perfectly co-ordinated with the phosphatases (especially PP2A) for correct mitotic entry, progression and exit. In this regard, it has been shown that cyclin B-Cdc2 is capable of phosphorylating and activating Gwl kinase in vitro (8) suggesting that cyclin B-Cdc2 itself would induce PP2A inhibition through Gwl activation (Fig. 4). Thus, it is possible that at mitotic entry, cyclin B-Cdc2 is first activated and this activation would further induce Gwl phosphorylation and activation. Accordingly, our data identified a pool of Gwl localized at the centrosome during G2 phase, the same subcellular and temporal localization where cyclin B-Cdc2 is first activated (20). Activated Gwl could subsequently induce PP2A inhibition permitting the correct phosphorylation of the different cyclin B-Cdc2 substrates. However, PP2A can also regulate cyclin B-Cdc2 activity, as the Wee1/Myt1 inhibitory kinases and the Cdc25 activatory phosphatase are themselves substrates of PP2A. Thus, the G2-arrest and the premature mitotic exit observed in Gwl knockdown cells are probably the result of both, a dephosphorylation of cyclin B-Cdc2 substrates and a subsequent inhibition of cyclin B-Cdc2 by Myt1/Wee1/Cdc25 dephosphorylation.

Therefore, cyclin B-Cdc2 kinase cannot be activated at mitotic entry if there is not first a partial inhibition of PP2A. This inhibition of PP2A could be mediated by a partial activation of Gwl through a cyclin B-Cdc2-independent phosphorylation of Gwl. Once cyclin B-Cdc2 is activated, it could act as the starter promoting full activation of Gwl and mitotic phosphorylation. The fact that cyclin B-Cdc2 could be one of the starters that promotes mitotic entry would assure that cells enter into mitosis only when a complete activation of this kinase is achieved.

Once cells enter into mitosis, Gwl-dependent inhibition of PP2A is still required to maintain the mitotic state. We have previously demonstrated that even in the presence of a high cyclin B-Cdc2 activity the substrates of this kinase become dephosphorylated and Xenopus egg extracts slip out of mitosis when PP2A cannot be inactivated by Gwl (11). Finally, at mitotic exit, cyclin B is degraded by the ubiquitin-dependent pathway promoting the inactivation of the cyclin B-Cdc2 complex. This inactivation results in the dephosphorylation of Gwl and the re-activation of PP2A. Once activated, PP2A induces dephosphorylation of mitotic substrates triggering an irreversible exit of mitosis until next G2 when cyclin B will accumulate again. Interestingly to date, mitotic slippage has been solely attributed to the slow continual degradation of cyclin B (21). However, from our results, premature activation of PP2A or loss of Gwl during mitosis is a new mechanism that could induce mitotic slippage independently of cyclin B degradation. This could have broad implication in defining new chemotherapies for cancer treatments that target the mitotic slippage pathway.

MATERIALS AND METHODS

Chemicals, Reagents and Antibodies

MG132 and Okadaic Acid were purchase from Calbiochem (La Jolla, CA). Anti-Cyclin B1 and Cdc2 (Santa Cruz, Santa Cruz, CA), anti-Phospho-(Ser) CDK Substrate and Phospho-Cdc2-Tyr15 (Cell signalling, Denver, MA), monoclonal 1D6 against PP2AC (Millipore

Temecula, CA), anti-Aurora B and BUBR1 (Becton Dickinson Franklin Lakes, NJ), and monoclonal anti-Gamma and ß-Tubulin (Sigma-Aldrich) were used. Anti-Cdc25 and Cdc27 were obtained as previously described (7, 19-22). pCMVsport6-MAST-L was obtained from RZPD Deutsches Ressourcenzentrum für Genomforschung GmbH, amplified by PCR and subcloned in the pGEX4T2 plasmid. The fusion protein was expressed in Escherichia coli. Inclusion bodies were prepared and used to immunize rabbits. Immune serum against the full-length protein (anti-hGwl) was affinity purified on an immobilized GST-MAST-L column. Anti-C-terminal hGwl antibodies were also generated against the last 12 aminoacids of the C-terminal sequence of this protein. Peptides were coupled to thyroglobulin for immunization and to immobilized bovine serum albumin for affinity purification as previously described (23).

Cell synchrony

Thymidine block/release synchronizations were performed as previously described (24). For Nocodazole synchrony, cells were first released from G1/S Thymidine block, and treated with 100 ng/ml of Nocodazole for 16 h. Floating cells were then removed, washed 3 times and seeded back in fresh media.

siRNA Design and Transfection

The Promega (Madison, WI) T7 Ribomax Express RNAi system was used to produce *in vitro* transcribed siRNAs against human Greatwall and PP2Ac. The following target sequences were identified and appropriate sense and anti-sense oligonucleotides were synthesized. For human Greatwall positions from #1=389-409, #2=840-860 and #3=1516-136. For PP2Ac, position #169-187, which targeted both α and ß isoforms. The following Scramble (SC) sequence was used SC=GGATTGTGCGGTCATTAAC, as a control. Transfection of siRNA was performed using Lipofectamine RNAiMax Reagent (Invitrogen) as per the manufacture's instructions. Rescue experiments were performed as per Figure S6. Briefly, synchronized

HeLa cells were first transfected with hGwl siRNA sequence #2 and subsequently transfected with a plasmid (PCS2) encoding full length Xenopus Gwl. Cells were synchronized, captured in mitosis with nocodazole, and analyzed by western blot.

Immunofluorescent Staining

Cells were grown on poly-lysine coated glass coverslips and pre- permeabilised for 30 seconds in PHEM buffer (60 mM PIPES, 25 mM HEPES, 1 mM EGTA, 2 mM MgCl2) + 0.25% Triton X-100. Then cells were fixed for 10 min in PHEM buffer with 3.7% formaldehyde and 0.5% Triton X-100, washed and blocked (3% BSA, 0,1% tween 20 in PBS) for 30 min. Primary antibodies were incubated for 2 h at RT in blocking solution. Images were captured using a Leica DM6000 microscope coupled with a Coolsnap HQ2 camera, using a Leica 63X APO 1.4 lens, powered by metamorph 7.1 software. For mitotic cells 0.3 m Z- sections were taken, and deconvoluted using Huygens 3.0 software. Maximum projections and total fluorescence measurements were performed with Image J, metaphase plate measurements and false coloring were performed using Photoshop CS4 Extended software.

Live cell imaging

Thymidine synchronized cells were filmed with a Micromax YHS 1300 camera coupled to a Zeiss Axiovert 200M inverted microscope fitted with a Zeiss slider PlasDIC 32X LD A plan NA 0.4 lens, Zeiss mercury lamp, and controlled by Metamorph 7.1 software (Molecular Devices, Sunnyvale, CA, USA). Images, both phase-contrast and GFP/CherryFP fluorescence, were taken every 10-15 min. The resulting images were processed, analyzed and false colored using Photoshop CS4 Extended software. Box Graphs and statistical analysis was performed using GraphPad Prism 5 (La Jolla, CA). Mitotic entry, length, exit, and cell death were determined as described in Figure S7. Briefly, the following parameters were used to identify mitotic entry: first appearance of a mitotic spindle with condensed chromosomes, loss of a nucleolus and rounding up of the cell from the culture plate. Exit was

scored based on the first appearance of anaphase, thus visualization of chromosome separation, pinching of the membrane and appearance of a mid-body.

ACKNOWLEDGMENTS

We thank Dr. J. Ellenberg and Dr. V Doye for the generous gift of the Hela EB3/H2B cell line, to Montpellier RIO Imaging for microscopy facilities and B. Gabrielli and K Rogowski for helpful comments on the manuscript. This work was supported by the Ligue Nationale Contre le Cancer (Equipe Labellisée, 2004-2008). A.B. and E.B. are "Fondation pour la Recherche Medicale" and "Ligue Nationale Contre le Cancer" fellows respectively.

ABBREVIATIONS

Gwl: Greatwall, **MAST-L:** Microtubule Associated Serine/Threonine Kinase Like, **SAC:** Spindle Assembly Checkpoint, **FACS:** Flow Cytometry Analysis, **PP2A:** Protein Phosphatase 2A, **OA:** Okadaic Acid, **CSF:** M-phase frog egg extracts, **SC:** Scramble.

REFERENCES

1. Jackman MR & Pines JN (1997) Cyclins and the G2/M transition. *Cancer Surv* 29**,** 47-73.
2. Bollen M, Gerlich DW, & Lesage B (2009) Mitotic phosphatases: from entry guards to exit guides. *Trends Cell Biol* 19**,** 531-541.
3. Mochida S, Ikeo S, Gannon J, & Hunt T (2009) Regulated activity of PP2A-B55 delta is crucial for controlling entry into and exit from mitosis in Xenopus egg extracts. *EMBO J* 28**,** 2777-2785.
4. Morgan DO (1997) Cyclin-dependent kinases: engines, clocks, and microprocessors. *Annual review of cell and developmental biology* 13**,** 261-291.
5. Glotzer M, Murray AW, & Kirschner MW (1991) Cyclin is degraded by the ubiquitin pathway. *Nature* 349**,** 132-138.

6. Bettencourt-Dias M, Giet R, Sinka R, Mazumdar A, Lock WG, Balloux F, Zafiropoulos PJ, Yamaguchi S, Winter S, Carthew RW, *et al*. (2004) Genome-wide survey of protein kinases required for cell cycle progression. *Nature* 432**,** 980-987.

7. Yu J, Fleming SL, Williams B, Williams EV, Li Z, Somma P, Rieder CL, & Goldberg ML (2004) Greatwall kinase: a nuclear protein required for proper chromosome condensation and mitotic progression in Drosophila. *The Journal of cell biology* 164**,** 487-492.

8. Yu J, Zhao Y, Li Z, Galas S, & Goldberg ML (2006) Greatwall kinase participates in the Cdc2 autoregulatory loop in Xenopus egg extracts. *Molecular cell* 22**,** 83-91.

9. Zhao Y, Haccard O, Wang R, Yu J, Kuang J, Jessus C, & Goldberg ML (2008) Roles of Greatwall Kinase in the Regulation of Cdc25 Phosphatase. *Mol Biol Cell*.

10. Castilho PV, Williams BC, Mochida S, Zhao Y, & Goldberg ML (2009) The M phase kinase Greatwall (Gwl) promotes inactivation of PP2A/B55delta, a phosphatase directed against CDK phosphosites. *Mol Biol Cell* 20**,** 4777-4789.

11. Vigneron S, Brioudes E, Burgess A, Labbe JC, Lorca T, & Castro A (2009) Greatwall maintains mitosis through regulation of PP2A. *EMBO J*.

12. Gandhi MJ, Cummings CL, & Drachman JG (2003) FLJ14813 missense mutation: a candidate for autosomal dominant thrombocytopenia on human chromosome 10. *Hum Hered* 55**,** 66-70.

13. Johnson HJ, Gandhi MJ, Shafizadeh E, Langer NB, Pierce EL, Paw BH, Gilligan DM, & Drachman JG (2009) In vivo inactivation of MASTL kinase results in thrombocytopenia. *Exp Hematol* 37**,** 901-908.

14. Janssens V & Goris J (2001) Protein phosphatase 2A: a highly regulated family of serine/threonine phosphatases implicated in cell growth and signalling. *Biochem J* 353**,** 417-439.

15. Beamish H, Deboer L, Giles N, Stevens F, Oakes V, & Gabrielli B (2009) Cyclin a/CDK2 regulates adenomatous poylposis coli dependent mitotic spindle anchoring. *J Biol Chem*.

16. Burgess A, Wigan M, Giles N, Depinto W, Gillespie P, Stevens F, & Gabrielli B (2006) Inhibition of S/G2 phase CDK4 reduces mitotic fidelity. *J Biol Chem* 281**,** 9987-9995.

17. Potapova TA, Daum JR, Pittman BD, Hudson JR, Jones TN, Satinover DL, Stukenberg PT, & Gorbsky GJ (2006) The reversibility of mitotic exit in vertebrate cells. *Nature* 440**,** 954-958.

18. Potapova TA, Daum JR, Byrd KS, & Gorbsky GJ (2009) Fine tuning the cell cycle: activation of the Cdk1 inhibitory phosphorylation pathway during mitotic exit. *Mol Biol Cell* 20**,** 1737-1748.

19. Vassilev LT, Tovar C, Chen S, Knezevic D, Zhao X, Sun H, Heimbrook DC, & Chen L (2006) Selective small-molecule inhibitor reveals critical mitotic functions of human CDK1. *Proc Natl Acad Sci U S A* 103**,** 10660-10665.

20. Jackman M, Lindon C, Nigg EA, & Pines J (2003) Active cyclin B1-Cdk1 first appears on centrosomes in prophase. *Nat Cell Biol* 5**,** 143-148.

21. Brito DA & Rieder CL (2006) Mitotic checkpoint slippage in humans occurs via cyclin B destruction in the presence of an active checkpoint. *Curr Biol* 16**,** 1194-1200.

FIGURE LEGENDS

Figure 1: hGwl siRNA knockdown induces multiple mitotic defects

(A) HeLa cells were synchronized by either Thymidine (Thy) or Nocodazole (Noc) shake-off, and released into fresh media. Samples were collected at the indicated times, and processed for western blot. Cell synchrony was confirmed by FACS. **(B)** HeLa cells were probed with anti-hGwl (green), anti-ß-tubulin (red) and DAPI (DNA, blue). The maximum projections from 0.3 μm

Z-sections are shown. Yellow arrows indicate the centrosomal localization of hGwl. Scale bar, 5 µm. **(C)** Enlargements of HeLa cells treated as per (B). Cells were counterstained with gamma-(interphase, red) or ß-tubulin (mitotic, cytokinesis, red), hGwl (green) and DNA (blue).

(D) Asynchronous HeLa cells were transfected with the indicated amounts of hGwl siRNA for 24 h and harvested immediately (24h) or 1 day later (48h). The levels of hGwl were analysed by western blot. **(E)** Asynchronous Hela cells were transfected with 50 nM of siRNA and analyzed by immunofluorescence with anti-hGwl antibodies. Arrow indicates a non-transfected cell **(F)** HeLa cells were treated as per (D) with either 50 nM of Scramble or hGwl siRNA and analysed by FACS. **(G)** Asynchronous HeLa cells treated as in (D) were analyzed by immunofluorescence. For ß-tubulin (red) and DAPI (DNA, blue). Scale bar, 5µm

Figure 2: hGwl knockdown promotes heterogeneity of phenotypes of varying severity in human cells

(A) HeLa cells stably expressing EB3-GFP (green) and H2B-CherryFP (red) were transfected with 50 nM of Scramble (Control) or hGwl siRNA for 24 h. After transfection, cells were synchronized with thymidine block. Movies were started 5 h post-release, and images were taken every 15 min. Notations indicate, time of the frame in minutes (white), lagging chromosomes (yellow arrows), metaphase plate orientation (dotted white lines) and cell death (yellow d). Scale bar, 5 µm. **(B)** Mitotic HeLa cells were treated with scramble or hGwl siRNA, and stained with anti-Aurora B or anti-BubR1 (red) antibodies and with DAPI (DNA, blue). Shown are the deconvoluted maximum projections from 0.3 µm Z- sections. Scale bar, 5 µm. **(C)** Cells from (A) were separated according to their mitotic phenotype and plotted against mitotic length. Mitotic entry was determined by analysing the first signs of DNA condensation cross-reinforced with cell rounding. Mitotic exit was scored based on chromosome segregation at anaphase and/or DNA decondensation. Shown are box-plots with 5-95% confidence intervals. Two-tailed unpaired student t-tests were performed to determine statistical relevance; significant p values are shown.

Figure 3: hGwl knockdown phenotypes can be rescued by the inactivation of PP2A

(A) Cells treated with increasing doses of hGwl siRNA were analysed by time-lapse microscopy as in Fig. 2A. The mitotic population was then scored on different criteria: cells that performed a correct mitosis (Normal) and cells that displayed the various aberrant phenotypes (No Metaphase Plate, Metaphase Arrest, Metaphase Delay and Segregation Defects). **(B)** Shown are box-plots for the mitotic length (right panel) in non-transfected cells (Lipo) and cells transfected with scramble siRNA (SC) or increasing doses of hGwl siRNA (25, 50 and 100 nM). Mitotic entry and exit was determined as in Fig.2. The small percentage of siRNA treated cells that completed mitosis correctly was not included in the analysis as these were likely to be un-transfected cells. The total number of cells observed in each condition is listed (N). **(C)** Similar to (B) except that the time of mitotic entry instead to the mitotic length was measured. **(D)** Hela cells were transfected with 100 nM of siRNA and synchronized with thymidine. The number of cells at S, G2 and mitosis at the indicated times was measured by 2D-FACS (Propidium Iodide versus anti-Phospho Ser Cdk1 staining). In one instance cells were released and treated with nocodazole (100 ng/ml) for 10 hours to capture the mitotic population (10+N). **(E)** HeLa cells were transfected or not (Lipo) with scramble (SC) or increasing amounts of siRNA (25, 50 and 100 nM), synchronized by thymidine and released into nocodazole (100 ng/ml) for 16 h. The phosphorylation of the different cyclin B-Cdc2 substrates (pSer) as well as the levels of cyclin B1, hGW and Cdc2 were analysed. The pSer staining was equalized against Cdc2 and the percentage of staining in each condition is indicated. **(F)** Hela cells were transfected with 50 nM of siRNA, synchronised by thymidine and 16 hours later analysed by immunofluorescence using anti-β-tubulin (red), anti-phospho Ser antibodies and DAPI for DNA (blue). Cells were separated into the various mitotic phenotypes observed: normal metaphase (Meta), metaphase with uncongressed chromosomes or undercondensed chromatin scattered along the spindle (Medium) or cells that underwent mitotic exit (Severe). Identical acquisition exposure time conditions were used to capture images. The intensity of staining

obtained with anti-phospho Ser antibody was measured in each unaltered cell and displayed as box-plots with 5-95% confidence intervals. Two-tailed unpaired student t-tests were performed to determine statistical relevance; significant p values are shown. **(G)** HeLa cells were transfected with 100 nM of human Greatwall (hGwl), PP2AC (P) or both human Greatwall and PP2AC (P+G) siRNAs. The pSer was equalized against ß-tubulin. Percentage of phosphorylation of the single hGwl knockdown (hGwl) was compared to scramble siRNA knockdown (SC), whereas, the percentage of phosphorylation of the double PP2AC/hGwl knockdown (P+G) was compared to single PP2AC knockdown (P). FACS analysis confirmed that the majority of cells were arrested in G2/M. **(H)** EB3-GFP (green) and H2B-CherryFP cells were transfected with 100 nM of scramble (SC) or hGwl siRNA (GW) and 24h later, synchronized with thymidine. Six hours after release cells were treated (SC+OA and Gwl+OA) or not (SC and Gwl) with 500 nM of OA and followed by time-lapse microscopy with images captured every 10 minutes. Time of mitotic entry was determined by DNA condensation and cell detachment in each cell and displayed as box-plots with 5-95% confidence intervals. Two-tailed unpaired student t-tests were performed to determine statistical relevance; significant p values are shown.

Figure 4: Hypothetical model showing the different steps required for mitotic entry

During G2 cyclin B is synthesised and accumulates to form a cyclin B-Cdc2 complex. At this phase of the cell cycle cells present a high PP2A activity. Wee1/Myt1 and Cdc25 are all substrates of PP2A. Dephosphorylated Wee1/Myt1 are active whereas dephosphorylated Cdc25 is inactive. Consequently cyclin B-Cdc2 is phosphorylated by Wee1/Myt1 kinases promoting its inactivity during G2. Although the exact mechanisms promoting entry into mitosis are unknown, it is likely that at mitotic entry, a cyclin B-Cdc2 independent phosphorylation of Gwl induces a partial inactivation of PP2A. This partial inactivation would allow a first burst of phosphorylation of Wee1, Myt1 and Cdc25 promoting the

activation of the cyclin B-Cdc2 amplification loop. Once activated cyclin B-Cdc2 will promote the complete phosphorylation of Gwl and the total inhibition of PP2A. Cyclin B-Cdc2 also promotes the phosphorylation of all the other mitotic substrates that now cannot be dephosphorylated by PP2A and therefore cells enter mitosis. Once in mitosis, PP2A activity must be inhibited to ensure that cyclin B-Cdc2 substrates remain phosphorylated long enough to performe mitosis correctly. This inhibition is assured by Gwl-dependent phosphorylation, which itself is maintained by cyclin B-Cdc2 activity. Finally, at metaphase-anaphase transition the ubiquitin-dependent degradation of cyclin B results in a loss of Cdc2 activity triggering Gwl dephosphorylation and inactivation, which then allows re-activation of PP2A. Once activated, PP2A will promote the irreversible dephosphorylation of mitotic substrates and cell will exit mitosis until next G2 phase in when cyclin B is synthesised again. Black arrows denote pathways active during mitotic entry. Dotted arrow denotes pathways that are inhibited at mitotic entry, during mitosis or at mitotic exit.

Figure 1

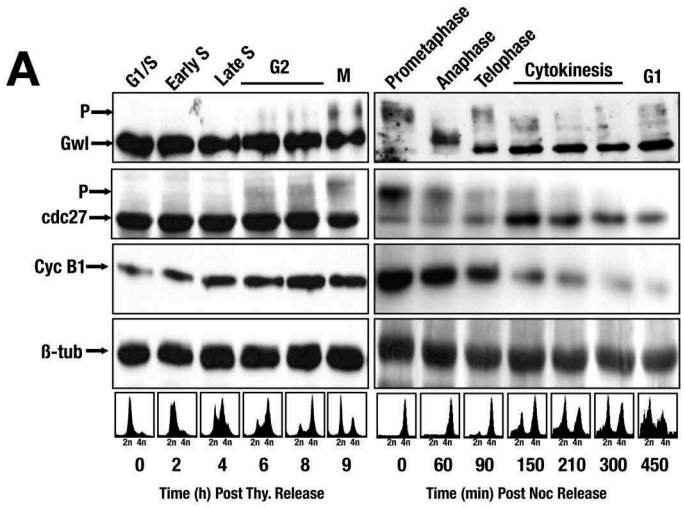
A
G1/S
Early S
Late S
G2
M
Prometaphase
Anaphase
Telophase
Cytokinesis
G1
P
Gwl
P
cdc27
Cyc B1
ß-tub
2n 4n
0 2 4 6 8 9
Time (h) Post Thy. Release
0 60 90 150 210 300 450
Time (min) Post Noc Release

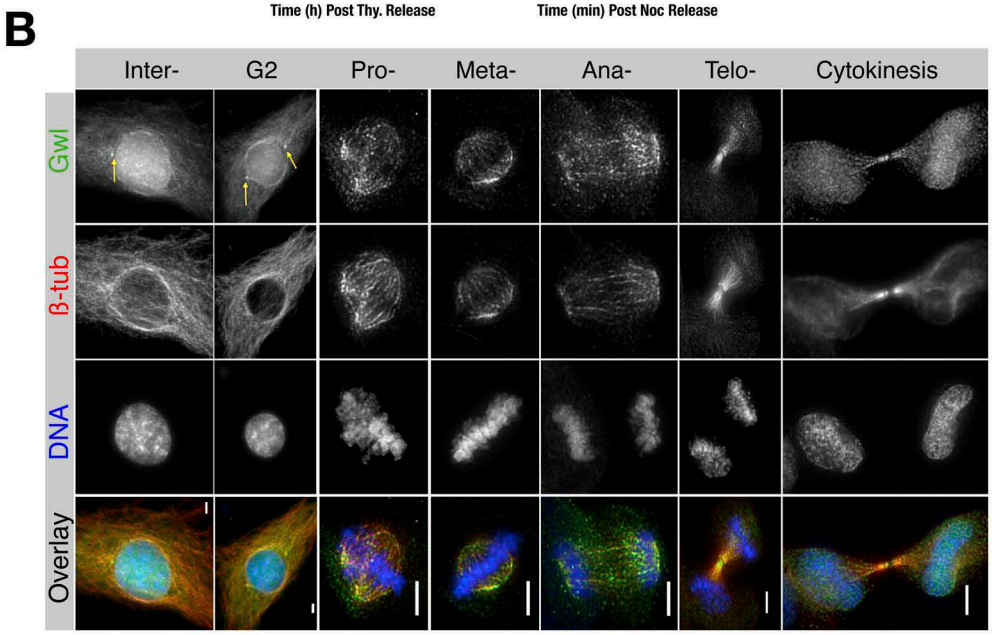
B
Inter-
G2
Pro-
Meta-
Ana-
Telo-
Cytokinesis
Gwl
β-tub
DNA
Overlay

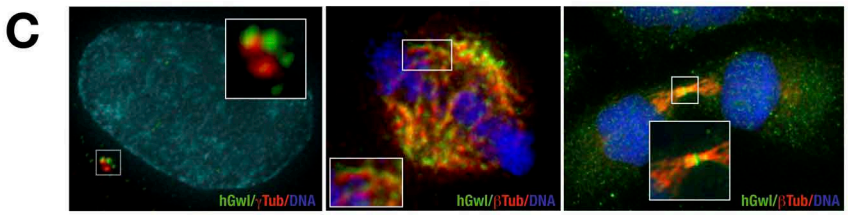
C
hGwl/γTub/DNA
hGwl/βTub/DNA
hGwl/βTub/DNA

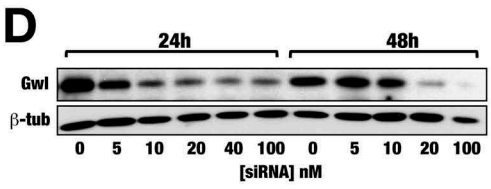
D
24h
48h
Gwl
β-tub
0 5 10 20 40 100 0 5 10 20 100
[siRNA] nM

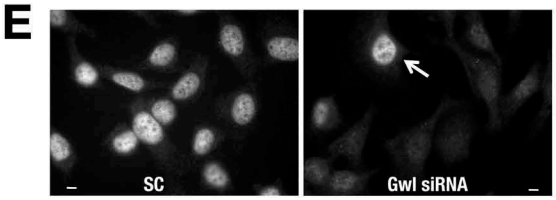
E
SC
Gwl siRNA

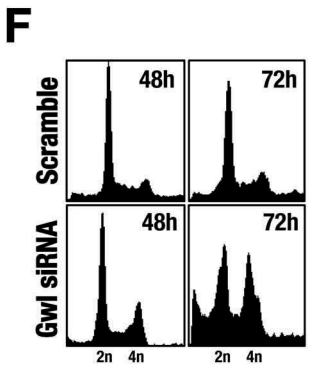
F
Scramble
48h
72h
Gwl siRNA
48h
72h
2n 4n
2n 4n

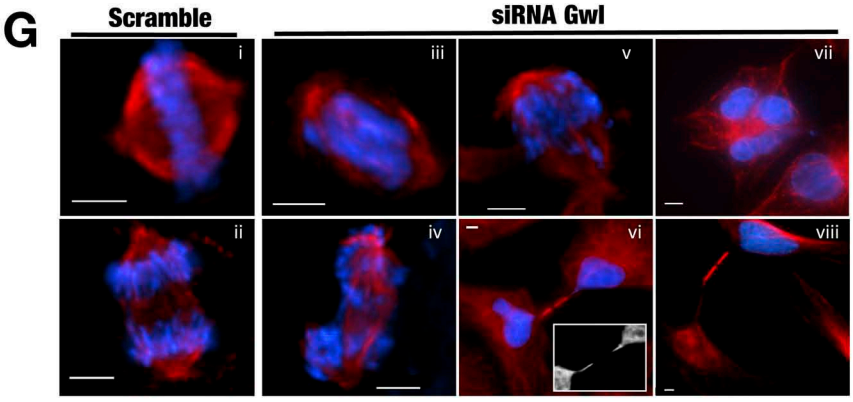
G
Scramble
siRNA Gwl
i
iii
v
vii
ii
iv
vi
viii

Figure 2

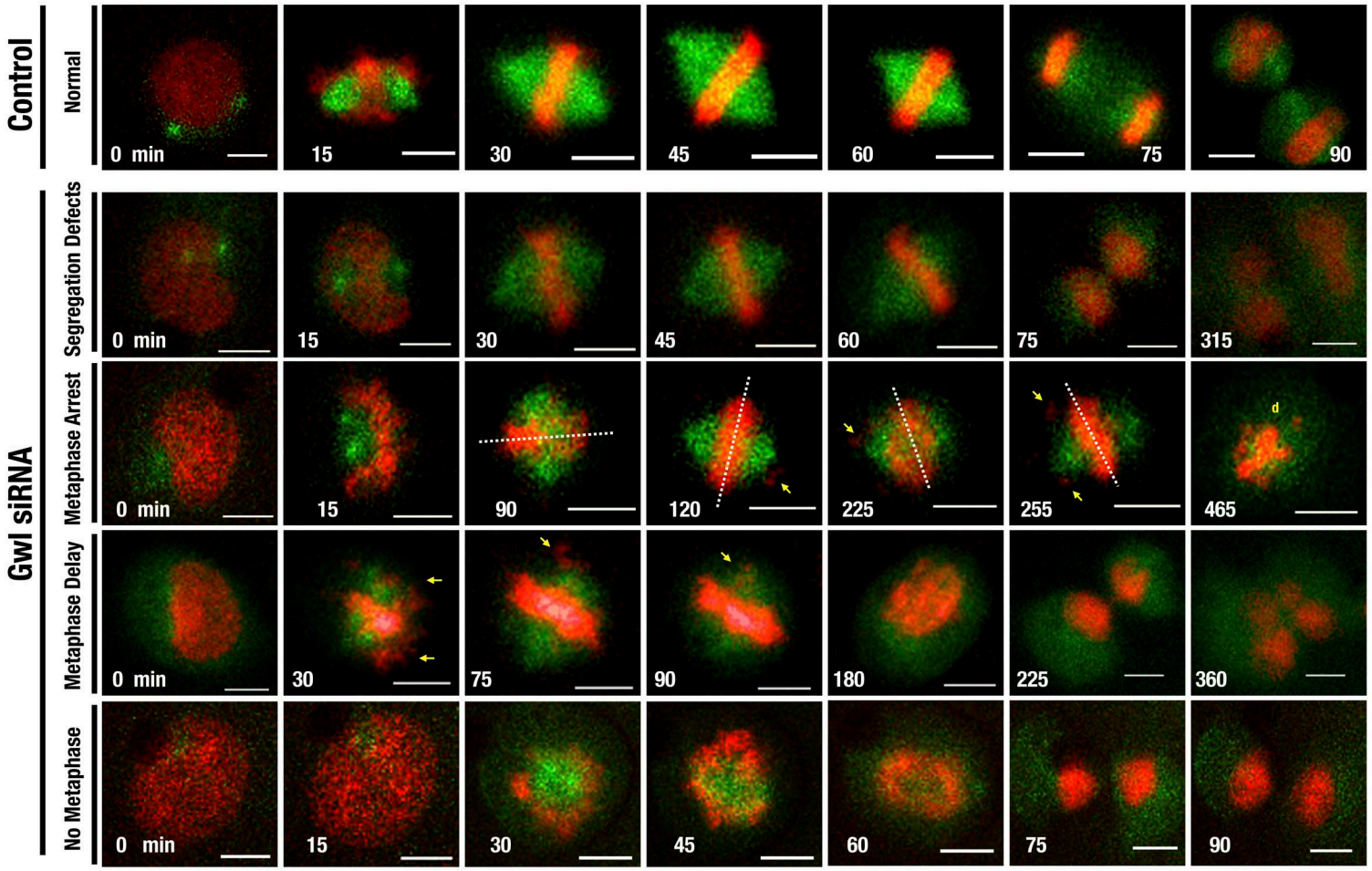
A
Control
Normal
Gwl siRNA
Segregation Defects
Metaphase Arrest
Metaphase Delay
No Metaphase
0 min
15
30
45
60
75
90
315
120
225
255
465
180
360
d

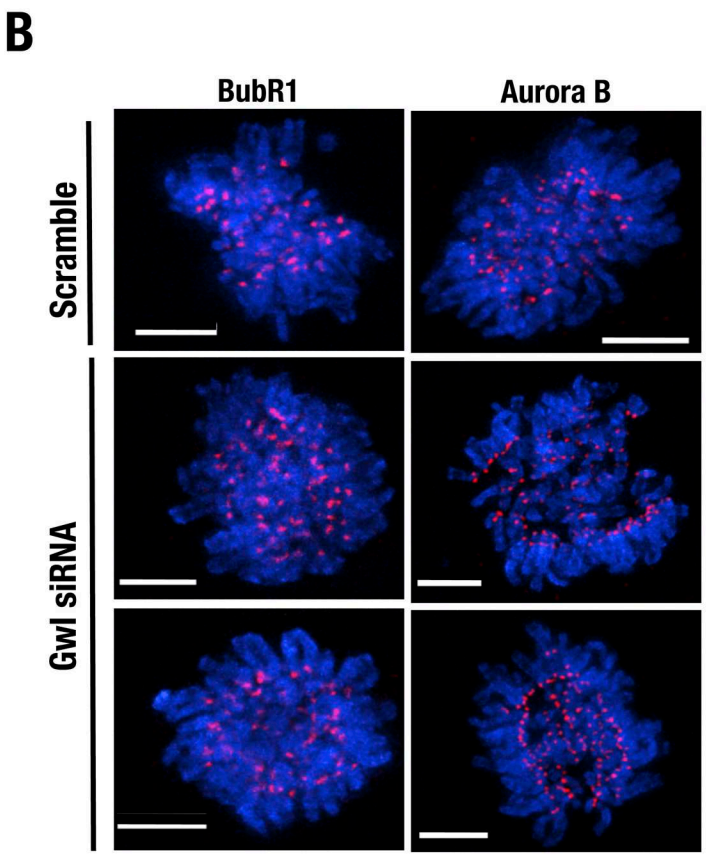
B
BubR1
Aurora B
Scramble
Gwl siRNA

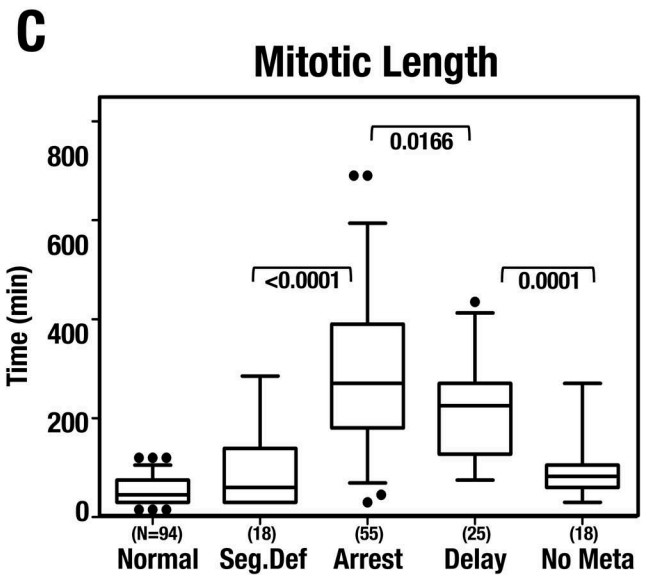
C
Mitotic Length
Time (min)
800
600
400
200
0
0.0166
<0.0001
0.0001
(N=94)
(18)
(55)
(25)
(18)
Normal
Seg.Def
Arrest
Delay
No Meta

Figure 3

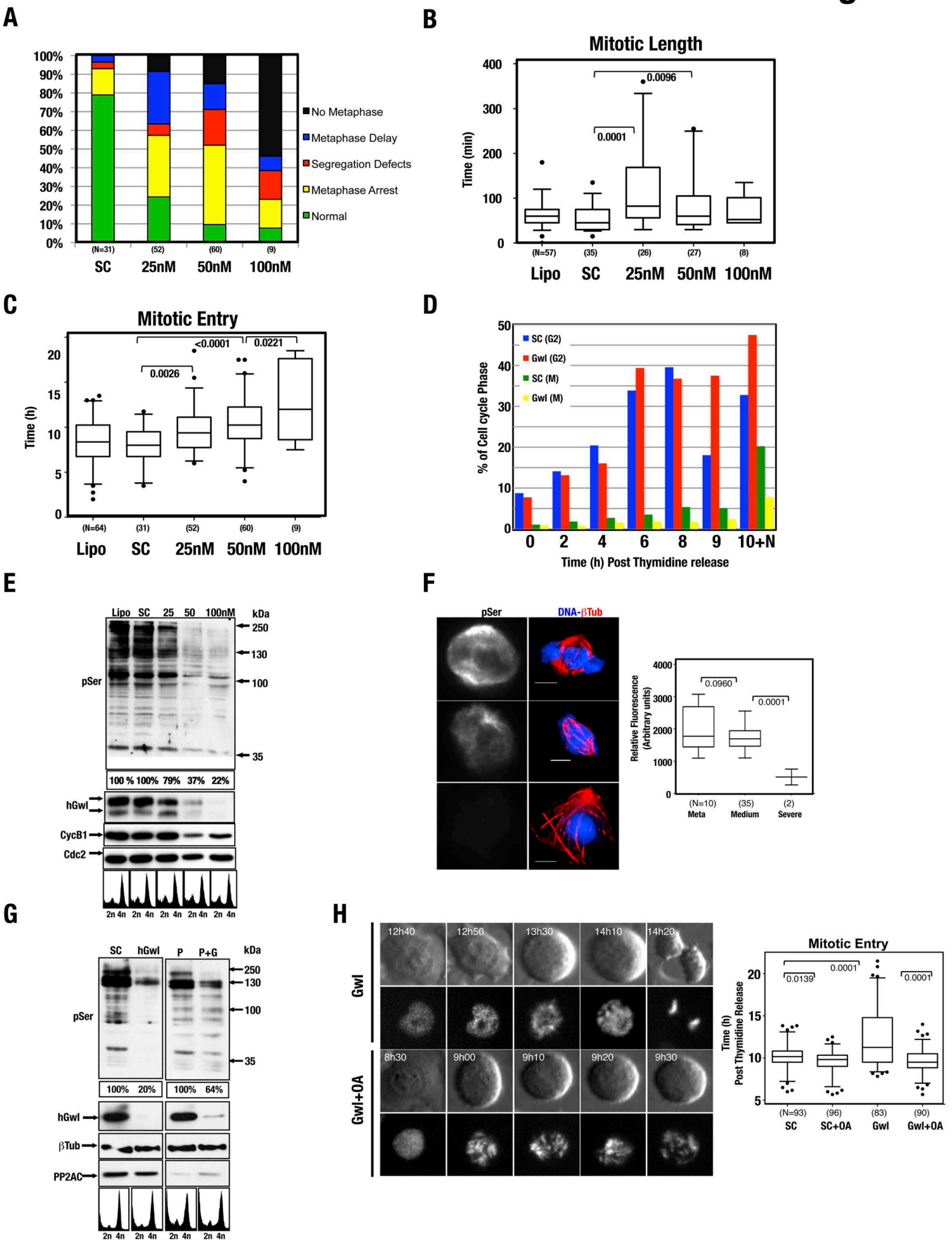
A
100%
90%
80%
70%
60%
50%
40%
30%
20%
10%
0%
No Metaphase
Metaphase Delay
Segregation Defects
Metaphase Arrest
Normal
(N=31)
(52)
(60)
(9)
SC
25nM
50nM
100nM
B
Mitotic Length
Time (min)
400
300
200
100
0
0.0096
0.0001
(N=57)
(35)
(26)
(27)
(8)
Lipo
SC
25nM
50nM
100nM
C
Mitotic Entry
Time (h)
20
15
10
5
0
<0.0001
0.0221
0.0026
(N=64)
(31)
(52)
(60)
(9)
Lipo
SC
25nM
50nM
100nM
D
% of Cell cycle Phase
50
40
30
20
10
0
SC (G2)
Gwl (G2)
SC (M)
Gwl (M)
0
2
4
6
8
9
10+N
Time (h) Post Thymidine release
E
Lipo
SC
25
50
100nM
kDa
250
130
100
35
pSer
100 %
100%
79%
37%
22%
hGwl
CycB1
Cdc2
2n 4n
F
pSer
DNA-βTub
Relative Fluorescence (Arbitrary units)
4000
3000
2000
1000
0
0.0960
0.0001
(N=10)
(35)
(2)
Meta
Medium
Severe
G
SC
hGwl
P
P+G
kDa
250
130
100
35
pSer
100%
20%
100%
64%
hGwl
βTub
PP2AC
2n 4n
H
Gwl
12h40
12h50
13h30
14h10
14h20
Gwl+OA
8h30
9h00
9h10
9h20
9h30
Mitotic Entry
Time (h) Post Thymidine Release
20
15
10
5
0.0139
0.0001
0.0001
(N=93)
(96)
(83)
(90)
SC
SC+OA
Gwl
Gwl+OA

Figure 4

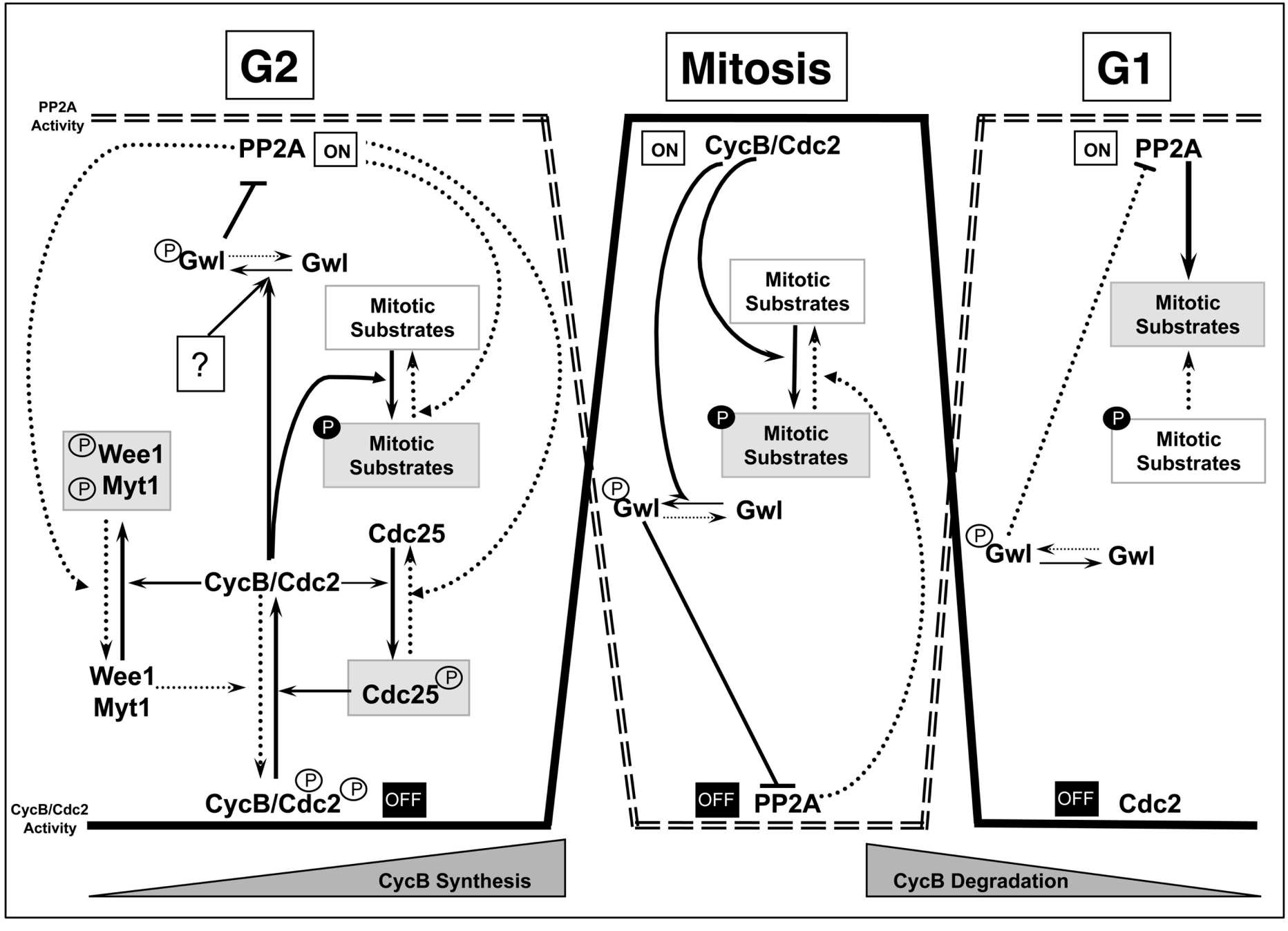
G2
Mitosis
G1
PP2A Activity
PP2A
ON
Gwl
Gwl
?
Mitotic Substrates
Mitotic Substrates
Wee1
Myt1
Cdc25
CycB/Cdc2
Wee1
Myt1
Cdc25
CycB/Cdc2
OFF
CycB/Cdc2 Activity
ON
CycB/Cdc2
Mitotic Substrates
Mitotic Substrates
Gwl
Gwl
OFF
PP2A
ON
PP2A
Mitotic Substrates
Mitotic Substrates
Gwl
Gwl
OFF
Cdc2
CycB Synthesis
CycB Degradation